Biosensors and Bioelectronics 144 (2019) 111675

Contents lists available at ScienceDirect

Biosensors and Bioelectronics

journal homepage: www.elsevier.com/locate/bios

A sensitive and selective approach for detection of IL 1α cancer biomarker using disposable ITO electrode modified with epoxy-substituted polythiophene polymer

Muhammet Aydın

Tekirdağ Namık Kemal University, Scientific and Technological Research Center, Tekirdağ, Turkey

ARTICLE INFO

Keywords:
Epoxy-substituted polythiophene
Interleukin 1α
Electrochemical impedance spectroscopy
Conjugated polymer

ABSTRACT

A highly sensitive and label-free electrochemical immunosensor for sensitive detection of interleukin 1α cancer biomarker was described by using epoxy-substituted polythiophene polymer modified disposable indium tin oxide electrode. This conjugated polymer was synthesized to fabricate this immunosensor for the first time and it offered a good biosensing platform for anti-IL 1α antibody immobilization due to epoxy groups present on the side groups of the polymer. Furthermore, the epoxy-substituted polythiophene polymer coated indium tin oxide electrode was used for the determination of IL 1α antigen for the first time. Electrode fabrication stages were characterized by using electrochemical (electrochemical impedance spectroscopy and cyclic voltammetry) and morphological (scanning electron microscopy and atomic force microscopy) techniques. Under optimum experimental conditions, impedimetric responses of the immunosensor increased with the increasing of IL 1α antigen concentration, and the proposed immunosensor displayed a wide linear detection range from 0.01 pg/mL to 5.5 pg/mL with a detection limit of 3.4 fg/mL. The proposed immunosensor exhibited outstanding performance including excellent reproducibility, good repeatability, high selectivity and long storage stability. With the advantages of simple operation, low-cost fabrication and label-free format, the suggested immunosensor was expected to have potential applications for IL 1α cancer biomarker detection.

1. Introduction

The early diagnosis and effective treatment of cancer disease are hot topics in clinical researches. Early diagnosis of cancer can save people's live and reduce the mortality rate. The detection of cancer biomarkers in human biological fluids is an effective approach for early diagnosis of cancer. In addition, cancer biomarkers detection offers the opportunities for understanding the main biochemical reactions occurred during disease progression (Zhang et al., 2014). Immunoassays, based on the feature of specific biorecognition of antigens by antibodies, are the most frequently utilized techniques in molecular diagnostics (Chen et al. 2019a, 2019b; Wang et al., 2018; Shi et al., 2018). Radioimmunoassay, chemiluminescence immunoassay, enzyme-linked immunosorbent assay (ELISA), and fluoroimmunoassay are usually used for cancer biomarkers detection (Li et al., 2010). These methods give reliable results, but they have some drawbacks such as having multistep procedure and long analysis duration, requiring highly trained personnel and high-cost devices (Aydın et al., 2019b). Therefore, development of simple and suitable methods for cancer biomarkers determination has gained attention. Electrochemical immunosensors are useful analytical techniques due to their excellent sensitivity, simple instrumentation, low cost, and high stability (Tang et al., 2011). Despite many advances in the development of electrochemical immunosensors, new biosensor fabrication strategies are required for the improvement of the sensitivity and selectivity. Great efforts have been made worldwide to develop portable electrochemical immunosensor enabling on-site analysis (Zhang et al., 2012; Zhang and Ren 2013).

Interleukin-1 (IL-1) is known as a main cytokine of inflammation (Dinarello et al., 2012) and it was discovered in the late 1970s. Since its discovery, IL-1 cytokine has attracted interest in several physiological processes and diseases. IL-1 mediates the local and systemic inflammatory processes and protects immunity against infections. Additionally, IL-1 has a significant role in homeostatic equilibrium. IL-1 family contains 11 cytokines (IL-1 to IL-11). IL-1α and IL-1β proteins are important for the pathogenesis of various solid tumors and hematological malignancies. In addition, IL-1 plays a protective role in immune responses during anticancer treatment (de Mooij et al., 2017). Interleukin 1α (IL 1α) is a cytokine and it includes 159 amino acids. The main role of IL 1α protein is regulation of the immune system (Park and Barbul 2004), inflammatory processes, hematopoiesis, and

E-mail addresses: muhammetaydin@nku.edu.tr, mhmmtaydin@outlook.com.

https://doi.org/10.1016/j.bios.2019.111675
Received 17 July 2019; Received in revised form 26 August 2019; Accepted 3 September 2019
Available online 06 September 2019
0956-5663/

nociceptive neurotransmission (Honore et al., 2006). It has role in different biochemical processes and promotes the cell growth (Wu et al., 2007). This cytokine is produced by activated macrophages, neutrophils, and epithelial and endothelial cells (Cervin Serrano et al., 2014). In addition, IL-1α is a tumor marker of oral squamous cell carcinoma (Mishra, 2012), head and neck squamous cell cancer (Polanska et al., 2014; Russo et al., 2016), and tongue cancer (Korostoff et al., 2011). The ranges of IL-1α biomarker in oral squamous cell carcinoma patients were 0–137 pg/mL in serum and 175–1000 pg/mL in saliva (Hamad et al., 2011). Because of the biological and pathological status of IL 1α biomarker, a great attention is found in determination of this tumor marker (Wu et al., 2007). For IL 1α biomarker detection, ELISA kits and biosensors are usually utilized. However, there are not many biosensors in the literature for the determination of IL 1α antigen (Tables SI–1) (Aydın and Sezgintürk 2019; Tao et al., 2006; Wu et al. 2006, 2007). Therefore, the proposed immunosensor is very important.

Electrochemical impedance spectroscopy (EIS) has attracted attention for investigation of biorecognition reactions that generated on the biosensor surface. The impedance of a biosystem is changed as a function of applied voltage and this impedance value is an indicator of interfacial changes (Lisdat and Schäfer 2008; Pänke et al., 2007). Biomolecule-functionalized support surfaces are significant in analyte biorecognition in biosensing system (Katz and Willner 2004; Wang and Hasebe 2009). The selection and preparation of interface material are important in the fabrication of electrochemical immunosensors (Palecek and Bartosik 2012). Conducting polymers have unique properties as electrode materials but they are not the only electrode materials used in sensors and biosensors (Ramanavičius et al., 2006). They are usually utilized in energy storage, memory devices and electrocatalysts (Rahman et al., 2008). Conjugated polymers are usually utilized to modify working electrode surfaces during chemo- or biosensing applications (Malinauskas et al., 2005; Moon et al., 2018). In order to enhance the application of conjugated polymers into the area of biosensors, one approach is to introduce functional groups, including carboxylic acid, amine, sulfonate, epoxy or thiol groups, to the side groups of conjugated polymers. These functional groups containing conjugated polymers have been successfully employed for biorecognition molecules immobilization during the biosensor development (Janmanee et al., 2012). In addition, conjugated polymers are considered as biocompatible materials in biological system because of their less/nontoxic effect. This property makes them an ideal matrix material for biosensor construction. Polythiophene is a polyaromatic and conjugated polymer, and it is usually utilized in biosensing applications because of its biocompatibility and stable property (Diaz et al., 1988; Feng et al., 2013). Polythiophene polymers have remarkable stability and they are suitable materials for the construction of immunosensors. The epoxy-substituted-polythiophene polymer (PThiEpx) is one of the conjugated polymers, which possess a lot of epoxy groups on its side groups. With its epoxy-groups, polymer can bind directly to the NH_2 groups of antibodies (Festag et al., 2005). Thus, antibodies bind to epoxy functionalized substrate via a two-step procedure including adsorption and covalent reactions between nucleophilic groups (amino) on antibody and epoxy groups on the surface (Vashist and Luong 2018). For the preparation of polythiophene polymer modified electrode surface, electrochemical polymerization technique has been mostly used in literature (Pilo et al., 2018; Plante et al., 2013; Védrine et al., 2003). In this study, spin-coating method was used instead of the electrochemical polymerization method for bioelectrode preparation. Spin-coating is a cost-effective method for highly sensitive biosensors development. The basic principle of spin-coating technique is based on deposition of a small drop of fluid on the flat substrate via centrifugal force. Because of centrifugal force, a reproducible and uniform surface is formed on the flat substrates. This method offers numerous advantages in fabrication of biosensors. In addition, this method is easy to use, and therefore, this method can be used with a wide variety of materials (Aydın et al., 2018b, c; Xu et al., 2010).

In the present study, a sensitive and label-free electrochemical immunosensor based on epoxy-substituted-polythiophene polymer (PThiEpx) modified disposable indium tin oxide-coated polyethylene terephthalate (ITO-PET) electrode was developed for the determination of IL 1α cancer biomarker. ITO-PET thin film was a unique material in terms of being disposable and low-cost, allowing different chemical modifications on the surface, and providing reproducible and highly accurate results. Therefore, ITO thin film was chosen as working electrode material. The polymer PThiEpx was used as an immobilization matrix to prepare a sensitive biosensor for the first time. Anti-IL 1α antibodies, which were biorecognition molecules, were immobilized on the polymer PThiEpx modified disposable ITO substrate covalently. Cyclic Voltammetry (CV) and EIS techniques were employed to characterize the immobilization process of functionalized immunosensor. Furthermore, scanning electron microscopy (SEM) and atomic force microscopy (AFM) measurements were used to monitor the modified electrode surfaces. By using this immunosensor, a new strategy with high sensitivity, good reproducibility, and low-cost features was developed for quantification of IL 1α tumor marker.

2. Experimental

2.1. Materials and reagents

3-Thiopheneacetic acid (98%, Sigma-Aldrich), glycidol (96%, Sigma-Aldrich), N-(3-dimethylaminopropyl)-N′-ethylcarbodiimide hydrochloride (EDCI.HCl), (≥98.0%, Sigma-Aldrich), 4-dimethylamino pyridine (≥99%, Merck) and anhydrous iron (III) chloride (97%, Merck) were employed as purchased without further purification. Nitromethane (98.5%, Merck), tetrahydrofuran (≥99.5%, Sigma-Aldrich), methanol (≥99.9%, Sigma-Aldrich), acetone (≥99.5%, Sigma-Aldrich), chloroform (≥99.5%, Sigma-Aldrich) and dimethyl sulfoxide (≥99.5%, Sigma-Aldrich) were used without further purification. Tetrahydrofuran (THF) was freshly dried by refluxing over sodium benzophenone ketyl under a dry argon atmosphere. Indium tin oxide coated polyethylene terephthalate film (ITO-PET) electrodes (5 mm × 20 mm, 60 Ω/cm^2), Anti-IL 1α antibody, IL 1α antigen, bovine serum albumin (BSA) were supplied by Sigma-Aldrich (USA). Anti-IL 1α antibody, IL 1α antigen and BSA (0.5%) solutions were prepared by using phosphate buffer (PBS, 50 mM, pH 7.4) and were kept at − 20 °C. Potassium chloride, sodium dihydrogen phosphate, di-sodium hydrogen phosphate, potassium ferrocyanide and potassium ferricyanide were obtained from Sigma-Aldrich (USA). All solutions were prepared using ultrapure water. Ferri-ferro solution was selected as the supporting electrolyte. Human serum samples were supplied by Tekirdağ Namık Kemal University, Faculty of Medicine with research ethics committee approval (2013/86/07/05). Neuron specific enolase, interleukin 1β, interleukin 8, and tumor necrosis factor α were chosen as interference biomarkers for examination of the specificity of the immunosensor.

2.2. Characterization and test equipment

FTIR Analysis: The infrared spectra of monomer, polymers and modified ITO electrode surfaces were recorded on a Bruker Company Vertex 70 spectrometer using ATR apparatus. FTIR spectra in the range 4000–400 cm^{-1} were recorded in order to investigate the nature of the chemical bonds.

DXR-Raman Analysis: The Raman characterization of monomer, polymers and modified ITO electrode surfaces were measured on a Thermo-Fischer Company DXR Raman spectrometer equipped with a 780-nm excitation laser wavelength. The RAMAN spectra were recorded in the range of 2000–400 cm^{-1} at a resolution of 4 cm^{-1}. Raman spectral data were analyzed by utilizing the Thermo Scientific OMNIC Software with an Array Automation function.

Proton NMR Analysis: The proton nuclear magnetic resonance

spectra were recorded in deuterated solvent ($CDCl_3$) using a 400 MHz Bruker Avance II spectrometer at room temperature. Chemical shifts of NMR were reported in ppm.

SEM and EDX Analyses: Scanning electron microscope images of ITO electrode surfaces were taken by utilizing Field Emission Scanning Electron Microscope (QUANTA FEG-250) with low vacuum detector (LFD). The working parameters (acceleration voltage:5 kV, spot size:3.5 and sample-to-detector distance:10 mm) were optimized to obtain the best possible resolution. The acceleration voltage and spot size were set to 30 kV and 6.0 for elementel mapping and spectral analysis with energy dispersive X-ray detector (EDX), respectively.

AFM Analysis: AFM images of ITO electrode surfaces in every modification stage were taken by employing a High-Performance Atomic Force Microscopy (hpAFM) NanoMagnetic Instrument. The scans of electrode surface were performed in tapping AFM mode under ambient conditions. The scan speed was 2 μm s^{-1} with a resolution of 256 pixels per line.

CV and EIS Analysis: Electrochemical measurements including EIS and CV were performed out with a Gamry Reference 1000 potentiostat/galvanostat. The three-electrode system, consisting of a platinum wire as an auxiliary electrode, Ag/AgCl as a reference electrode, and disposable ITO substrate as a working electrode, was utilized in this study. EIS and CV analyses were performed in the presence of 5 mM $K_3[Fe(CN)_6]/K_4[Fe(CN)_6]$ (1:1) mixture and 0.1 M KCl. In cyclic voltammetry measurements, the potential was recorded between −500 mV and 1000 mV (step size: 10 mV, scan rate: 100 mV/s). Electrochemical impedance measurements were carried out by applying an alternating potential of 5 mV to the working electrode. The formal potential applied in the impedance studies was 0 V. Another important parameter in impedance measurements was the frequency range from 50,000–0.05 Hz. In addition, EIS and CV measurements were recorded via EChem Analyst software program.

2.3. Synthesis of monomer and polymer

2.3.1. Synthesis of epoxy-substituted thiophene monomer (3-ThiEpx)

Epoxy functional group containing thiophene monomer (3-ThiEpx) was synthesized to reported procedure with minor modifications in steglich esterification method (Neises and Steglich 1978). The N-(3-dimethylaminopropyl)-N′-ethylcarbodiimide hydrochloride (EDCI·HCl) (1.917 g, 10 mmol), 4-dimethylamino pyridine (DMAP) (0.056 g, 0.5 mmol) and 3-thiopheneacetic acid (0.710 g, 5 mmol) were put into a 50-mL round bottom flask and were solved in dry tetrahydrofuran (THF, 35 mL). Then, glycidol (0.432g, 6 mmol) were added to reaction solution, and it was stirred at room temperature under inert gas for 2 days. After reaction, tetrahydrofuran was evaporated, and diethyl ether was added to extract. Then, the organic layer was carefully rinsed repeatedly with deionized water and brine solution. Finally, the organic layer was dried over anhydrous magnesium sulfate and it was concentrated in rotary evaporation for crude monomer production. Pure product was obtained as a colorless liquid. (Yield: %69.6, 0.69g). FTIR (ATR) cm^{-1}: 3058 (C–H aromatic); 2927, 2880 (C–H aliphatic); 1734(C═O); 1537; 1480; 1256; 1132; 1081; 946; 908; 856; 761 (C–S–C); 733; 699; 611 (Fig. SI-2). Raman ($\lambda_{laser=780\ nm}$): 2996, 2934 (-CH_2); 1737 (C═O); 1540; 1412; 1258; 1152; 1084; 1005; 947; 924; 860; 836; 677; 615 (Fig. SI-3). ^{1}H-NMR (δH, ppm) (400 MHz, $CDCl_3$): 7.29 ppm (Ha; 1H), 7.05 ppm (Hb; 1H), 7.17 ppm (Hc; 1H), 3.71 ppm (Hd; 2H), 4.46 and 3.95 ppm (He1,2; 2H), 3.21 ppm (Hf; 2H) and 2.84 and 2.63 ppm (Hg1,2; 2H) (Fig. SI-4).

2.3.2. Synthesis of epoxy-substituted polythiophene polymer (PThiExp)

Oxidative polymerization of epoxy-substituted thiophene monomer was performed using ferric chloride ($FeCl_3$) (Aydın et al., 2019a; David et al., 2019). Epoxy-substituted thiophene monomer (3-ThiEpx) (1.98 g, 0.1 mol) with anhydrous chloroform ($CHCl_3$; 70 mL) was added to a 100-mL three-neck round bottom flask equipped with a magnetic stirrer and rubber septum under argon gas. The reaction flask was cooled to −10/-15 °C utilizing an ice-salt mixture. Then, freshly prepared anhydrous $FeCl_3$ (6.48 g, 0.4 mol) solution in nitromethane (CH_3NO_2; 23 mL) was added dropwise via syringe through the septum to the mixture over a 20 min-period, and the mixture was stirred at room temperature for 2 h. The molar ratio of the oxidant to monomer was 4:1. The black polymer solution was concentrated to 10 mL by rotary evaporation and it was precipitated in large excess cold methanol. The orange polymer precipitate was collected by filtration, and it was purified by repeated rinsing with fresh methanol (using a Soxhlet apparatus) and ultrapure water to remove the residual $FeCl_3$ and the oligomers to yield the pure polymer. The polymer was dried in vacuum at 30 °C overnight. (Yield: %38.1, 0.75g). FTIR(ATR) cm^{-1}: 2960–2883(CH); 1722(C═O); 1550; 1450; 1400; 1251; 1163; 1130; 1040; 930; 841; 782; 745; 676; 621(Fig. SI-2). Raman ($\lambda_{laser=780\ nm}$): 2965, 2934 (CH); 1730 (C═O); 1488; 1333; 1235; 1034; 918; 850(Fig. SI-3).

2.4. Fabrication of the proposed immunosensor and electrochemical procedures

In the present study, polymer PThiEpx were prepared by oxidative polymerization reaction. The step-by-step development of the polymer-based immunosensor is displayed in Scheme 1. Before modification, an ITO substrate was successively washed with acetone, soap solution, and ultrapure water for 10 min in ultrasonic bath and dried under argon gas. The polymer PThiEpx was solved in mixed solvents (THF/DMSO/Acetone) and 30 μL PThiEpx polymer (0.5 mg/mL) was dropped on the clean ITO substrate surface and the ITO substrate was spin-coated to obtain homogenous electrode surface. Afterwards, the ITO substrate was dipped in a PBS solution containing 1.5 ng/mL of anti-IL 1α antibodies (100 μL in microcentrifuge tube) for 30 min to obtain ITO/PThiEpx/anti-IL 1α antibody bioelectrode. After antibody immobilization on the ITO substrate, ITO/PThiEpx/anti-IL 1α bioelectrode was immersed in BSA solution (100 μL in microcentrifuge tube) to block the free epoxy groups and incubated there for an hour. After washing thoroughly with ultrapure water, the obtained ITO/PThiEpx/anti-IL 1α/BSA functionalized ITO substrate was ready to IL 1α antigen measurement. Electrode preparation steps, optimization studies and analytical characteristics of designed immunosensor were performed following electrochemical methods, electrochemical impedance spectroscopy (EIS) and cyclic voltammetry (CV). All electrochemical experiments were performed in a solution containing 5 mM $K_3[Fe(CN)_6]/K_4[Fe(CN)_6]$ (1:1) as a redox probe. The redox probe solution also contained 0.1 KCl to decrease the resistance of probe solution. The impedance spectra were recorded in the frequency range 0.5 Hz-5x10^4 Hz. CV analyses were performed in a potential range from 0 to 500 mV at a scan rate 100 mV/s.

3. Results and discussion

Scheme 1 illustrates schematically the different steps implied in the preparation of ITO/PThiEpx/anti-IL 1α/BSA/IL 1α immunosensor. As it is explained in the electrochemical immunosensor preparation section (2.3), a sensitive immunosensor was constructed upon covalent coupling of anti-IL 1α antibody on polymer PThiEpx modified ITO substrate. The biorecognition interactions were investigated by EIS and CV measurements and the IL 1α concentration quantification was carried out also by impedimetric measurements.

3.1. Chemical characterization of the ITO electrode surface

Scheme 1 shows the chemical structures and synthesis routes of the thiophene monomer (3-ThiEpx) and epoxy-substituted conjugated polymers. The epoxy functional group substituted thiophene polymer was successfully synthesized by utilizing two-step reaction procedure

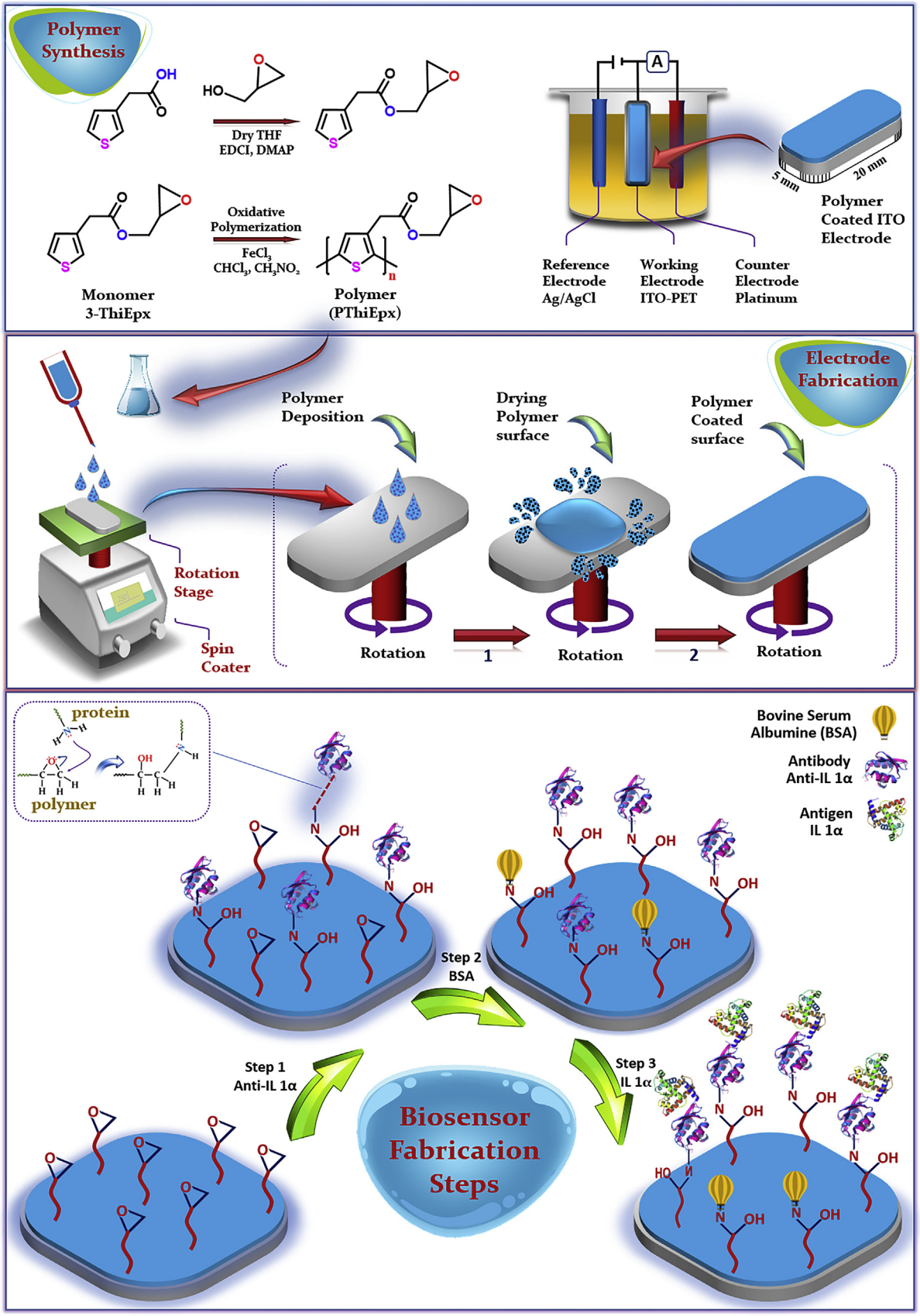

Scheme 1. Schematic illustration of fabrication steps applied to the disposable ITO electrode.

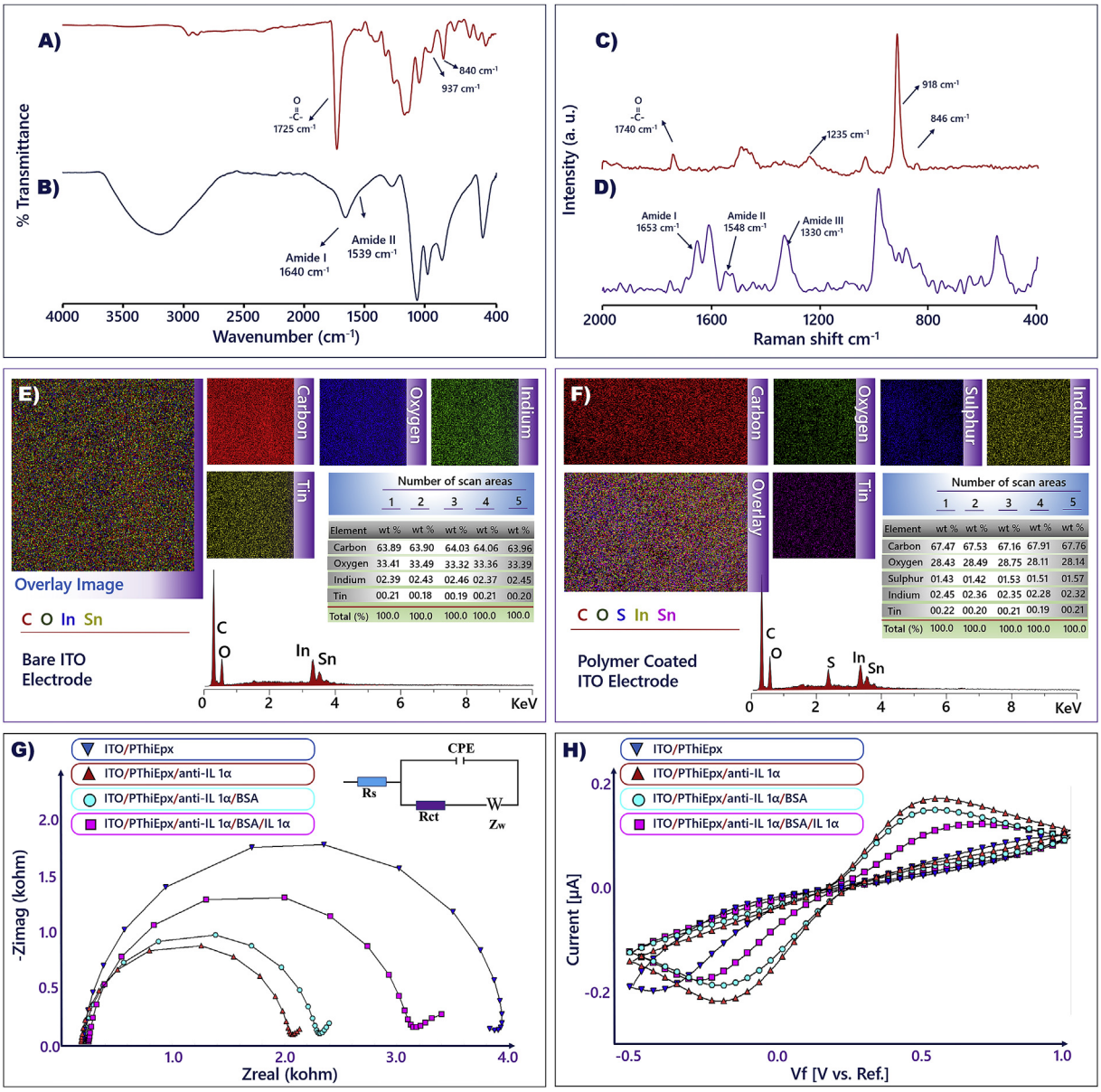

Fig. 1. Chemical characterization of the suggested immunosensor; FTIR spectrum of ITO/PThiEpx (A) and ITO/PThiEpx/anti-IL 1α (B), Raman spectrum of ITO/PThiEpx (C) and ITO/PThiEpx/anti-IL 1α (D), Elemental mapping and EDAX spectra of bare ITO electrode (E) and ITO/PThiEpx, electrode (F), EIS (G) and CVs (H) of fabrication steps.

consisting of esterification and oxidative polymerization technics. Initially, epoxy-substituted thiophene monomer (3-ThiEpx) was synthesized by steglich esterification reaction betwen 3-thiopheneacetic acid and glycidol in dry tetrahydrofuran. The steglich esterification was a mild reaction, which was one of the convenient methods for the formation of ester groups. Epoxy functional group containing conjugated polymer was synthesized according to classical chemical oxidative polymerization reaction. The synthesized chemical structures were characterized by FTIR, Raman and ^{1}H NMR spectroscopy to display the success of their synthesis techniques and to determine chemical structures of them. Also, the obtained results are illustrated in detail in the Supplementary information file. Fig. 1A and B shows FTIR spectra of polymer PThiEpx modified ITO electrode surface and anti-IL 1α immobilized ITO electrode surface, respectively. In the IR spectra of polymer modified electrode surface (red line), the characteristic vibrations of epoxy group in polymer were seen at 930 cm^{-1} and 841 cm^{-1} (Aydın et al., 2019a; Oh et al., 2010). Furthermore, the broad C–S–C asymmetric and symmetric stretching peaks at 1130 cm^{-1} and 745 cm^{-1} confirmed the presence of thiophene ring on the electrode surface. The strong and sharp signal seen around 1725 cm^{-1} was an evidence of the C=O stretching vibration of carbonyl groups (Aydın et al., 2018b). In the IR spectra of anti-IL 1α antibody immobilized electrode surface (blue line), broad and intense bands were seen for amide I at ~1640 cm^{-1} and for amide II at ~1539 cm^{-1}, and these bands clearly demonstrated the presence of the anti-IL 1α antibody immobilization onto polymer PThiEpx modified ITO electrode surface (Aydın et al., 2019c; Banas et al., 2015). FTIR and Raman are complementary spectroscopic techniques (Clemens et al., 2014). So, the chemical structures of polymer PThiEpx modified ITO substrate surface before and after anti-IL 1α antibody attachment were also investigated via Raman spectroscopy (Fig. 1C and D). The characteristic bands at 1240 cm^{-1}, 918 cm^{-1}, and 845 cm^{-1} confirmed the presence of the oxirane ring on the polymer PThiEpx modified ITO electrode surface (Fig. 1C) (Aydın et al., 2018b). Raman spectroscopy is an excellent tool for the protein structure investigation (Kuhar et al., 2018). Moreover, Raman spectral technique was an excellent and successful technique for

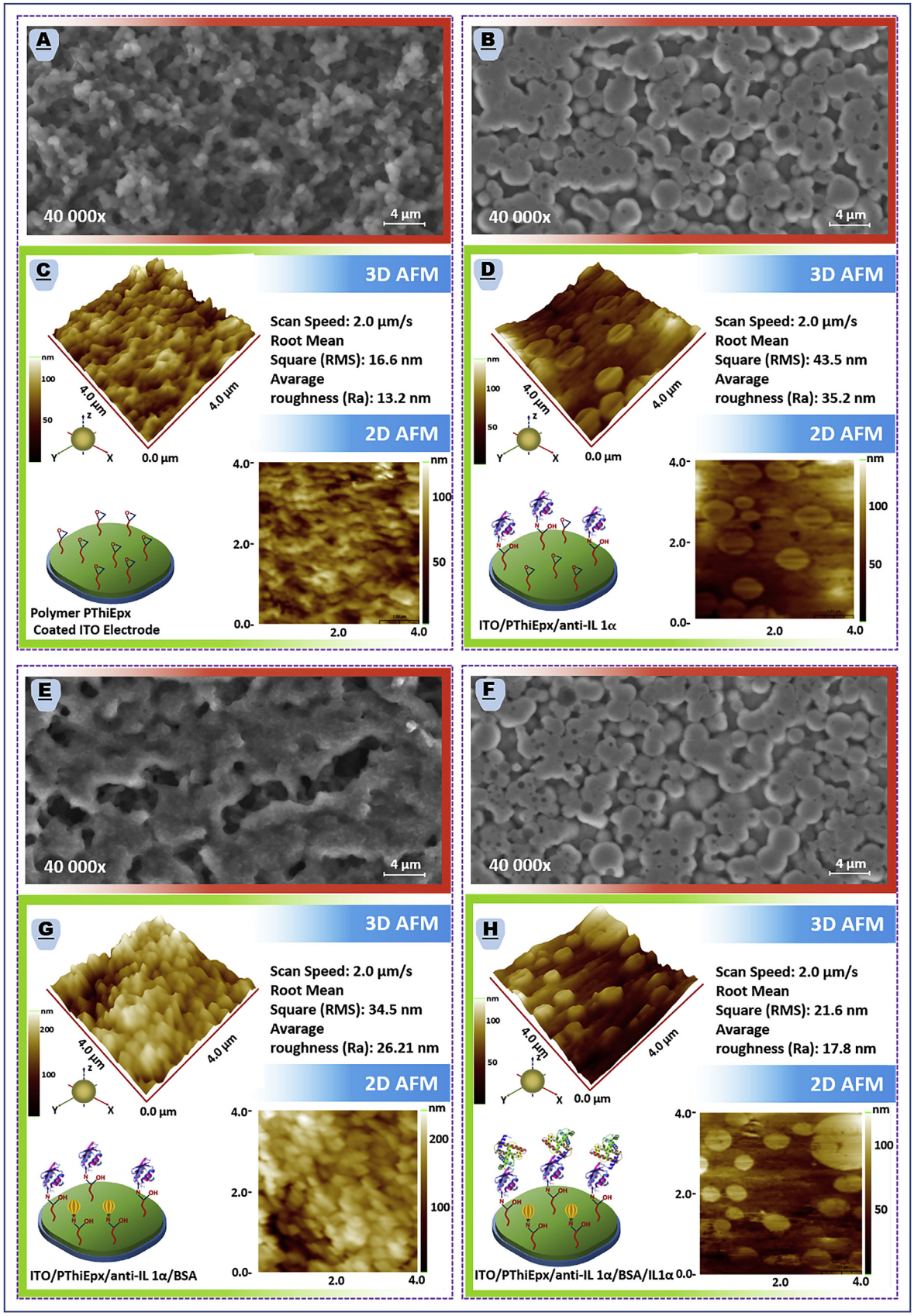

Fig. 2. SEM and AFM images captured from the surface of ITO/PThiEpx (A and C), ITO/PThiEpx /anti-IL 1α (B and D), ITO/PThiEpx/anti-IL 1α/BSA (E and G), ITO/PThiEpx/anti-IL 1α/BSA/IL 1α (F and H).

identifying amide bonds (Austin et al., 2016). The secondary structures of proteins such as amide I, II and III are mostly monitored between 1650 and 1680 cm^{-1}, 1480-1570 cm^{-1} and 1235-1300 cm^{-1}, respectively (Ghosh et al., 2019; Kitagawa and Hirota 2006; Panikkanvalappil et al., 2019). As shown in Fig. 1D, amide I, amide II and amide III bonds were found at 1653 cm^{-1}, 1548 cm^{-1} and 1330 cm^{-1}, respectively.

Energy-dispersive x-ray spectroscopy was used to determine the elemental composition of bare ITO electrode surface and polymer PThiEpx modified ITO electrode surface. As shown in Fig. 2E, bare ITO had carbon (C), oxygen (O), indium (In), and tin (Sn) elements and this result was compatible with literature (Aydın et al., 2018a). After polymer PThiEpx modification of ITO electrode, spectra contained carbon (C), oxygen (O), sulphur (S), indium (In), and tin (Sn) elements (Fig. 2F). In addition, the successful immobilization of polymer on ITO electrode surface was evidenced by the presence of a sulphur atom which was originated from the thiophene rings of polymer PThiEpx. Five different EDX-spectral analyses were performed to demonstrate homogeneous dispersion of the polymer on the electrode surface. The Sulphur atom ratio results were very close (S: 1.43%, 1.42%, 1.53%, 1.51%, 1.57%). The obtained result proved the abundance of the polymer PThiEpx on the ITO electrode surface.

3.2. Electrochemical characteristics of the proposed immunosensor

EIS is a sensitive technique to investigate the interfacial properties of the electrode modification steps. The impedance spectra consist of two parts; a semicircle portion at higher frequencies and a linear portion at lower frequencies. The electron transfer resistance (R_{ct}), which equals the semicircle portion, illustrates the electron transfer kinetics of the redox couple at the electrode interface. Each modification stage was analyzed by EIS technique and each electrochemical reaction is presented by an electric circuit. A Randles equivalent circuit include the solution resistance (R_s), the charge-transfer resistance (R_{ct}), the Warburg resistance (Z_w) and the constant phase element (CPE) (Bahadır and Sezgintürk, 2016).

Immunosensor fabrication was performed by proper modification of ITO substrate surface. After successful modifications, electrochemical characterization of the ITO substrate surface was performed using EIS and CV techniques. Fig. 2A shows EIS spectra of the IL 1α immunosensor fabrication steps, respectively. EIS analyses were performed to follow the change in electron transfer resistance (R_{ct}) of $[Fe(CN)_6]^{3-/4-}$ as redox couples. Modifying the ITO electrode surface with polymer PThiEpx provided a polymer layer on the ITO substrate surface and this polymer layer inhibited electron transfer and hence a high R_{ct} value was obtained. Anti-IL 1α antibody coupling on the polymer PThiEpx modified ITO substrate caused a decrease in R_{ct} value due to charge balancing on the epoxy groups of polymer PThiEpx. After that, the electrode surface was blocked for non-specific interaction by BSA, an increment in R_{ct} value was obtained, indicating that BSA layer hindered the electron transfer. Finally, an increase was observed at the R_{ct} value after IL 1α antigen immobilization. This increase displayed that IL 1α antigens were successfully captured by the immunosensor. All of the EIS spectra were fitted by a Randles equivalent circuit simulation via Gamry Software (Fig. 2A inset). In addition, CV measurements were also studied. Fig. 2B displays the CVs of the ITO electrode surface at every modification stage. The polymer PThiEpx modified ITO electrode had high peak currents owing to polymer layer formation on the ITO substrate surface. The peak currents increased after immobilization of anti-IL 1α antibodies and this increase might be due to rebalancing of charges on the epoxy groups. After BSA blockage step, decreases were observed in peak currents, which displayed the protein layer formation on the ITO electrode surface. When anti-IL 1α antibodies conjugated with IL 1α antigens, decreases in peak currents were seen, suggesting that a successful biorecognition event was formed. This biorecognition event resulted in an immunocomplex formation that obstructed the electron transfer to the electrode surface.

3.3. Surface morphological studies of the designed immunosensor

The change in the surface morphology of the working electrode upon modification with polymer PThiEpx, anti-IL 1α antibody, and IL 1α antigen was observed with using SEM and AFM analyses. As shown in Fig. 2A, the polymer had a uniform dispersion on the ITO substrate surface. The uniform distribution on the ITO electrode surface was also observed using the AFM imaging. This result showed that AFM image supported the SEM image. The surface roughness of polymer PThiEpx coated ITO surface was measured as 13.2 nm (Fig. 2C). As seen in Fig. 2B, anti-IL 1α antibodies were sphere like structures. Also, the surface morphology completely changed after IL 1α antibody attachment. An increase in surface roughness value (35.2 nm) proved the antibody immobilization on the ITO electrode surface (Fig. 2D). After antibody attachment step, the ITO electrode surface was modified with BSA to block the free epoxy groups of polymer PThiEpx. Fig. 2E shows the SEM image of ITO/PThiEpx/anti-IL 1α/BSA. The BSA layer on the ITO substrate surface was clearly observed. As seen in Fig. 2G, a smooth surface was obtained after BSA blockage step (surface roughness; 26.2 nm). After IL 1α antigen coupling on the modified ITO electrode surface, an immunocomplex was formed and this immunocomplex caused a change on the surface morphology (Fig. 2F). As seen in Fig. 2F, ITO electrode surface was completely coated with IL 1α antigens. The AFM image supported the SEM image (Fig. 2H) and this image indicated that the excessive amount of IL 1α antigen was present on the ITO substrate surface.

3.4. Optimization of the experimental parameters

To obtain optimal analytical performance of the suggested immunosensor, some experimental variables such as polymer concentration, anti-IL 1α antibody concentration, anti-IL 1α antibody incubation period, and IL 1α antigen incubation period were examined. During the optimization and analytical characterization experiments, a single calibration curve with 8 concentration levels were prepared by using 8 bioelectrodes. Furthermore, in the optimization experiments, each parameter measurement was repeated 3 times. The concentration of IL 1α antigen stock solution was 20 μg/mL. The calibration points (0.01 pg/mL, 0.11 pg/mL, 0.44 pg/mL, 0.77 pg/mL, 1.54 pg/mL, 2.2 pg/mL, 3.85 pg/mL and 5.5 pg/mL) were prepared by dilution of stock solution with PBS solution(50 mM pH 7.4). The amount of polymer used during the experiment was a significant parameter to acquire sufficient epoxy ends formation on the ITO electrode surface. Therefore, three different polymer levels (0.25 mg/mL, 0.5 mg/mL and 1 mg/mL) were used and the immunosensor responses were investigated. Low polymer concentration was not sufficient for the formation of epoxy groups, and a low immunosensor signal was obtained. The highest immunosensor signal was seen when 0.5 mg/mL of polymer PThiEpx was used. An increment in polymer level did not increase the immunosensor signal. The antibody immobilization condition was another essential parameter. To optimize the utilized antibody concentration, we studied three different antibody concentrations (0.3 ng/mL, 1.5 ng/mL and 3 ng/mL). If the antibody concentration was too high, it would lead to a waste; if too low, there would be too many unspecific sites on the electrode surface. As seen in Fig. 3B, a small amount of antibody attachment on the ITO substrate surface caused a low response and the maximum response was obtained when 1.5 ng/mL of anti-IL 1α antibody was used. At higher concentration (3 ng/mL), electrode surface degeneration probably started; and therefore, a low immunosensor response was obtained. Also, 1.5 ng/mL of anti-IL 1α antibody was selected as the optimum anti-IL 1α concentration. The incubation period was a significant parameter affecting the analytical features of electrochemical immunosensors. To obtain optimum antibody incubation period, the ITO electrodes were incubated in anti-IL 1α antibody solutions for different amounts of time (30 min, 45 min, and 60 min). Fig. 3C displays the immunosensor signals after 30 min,

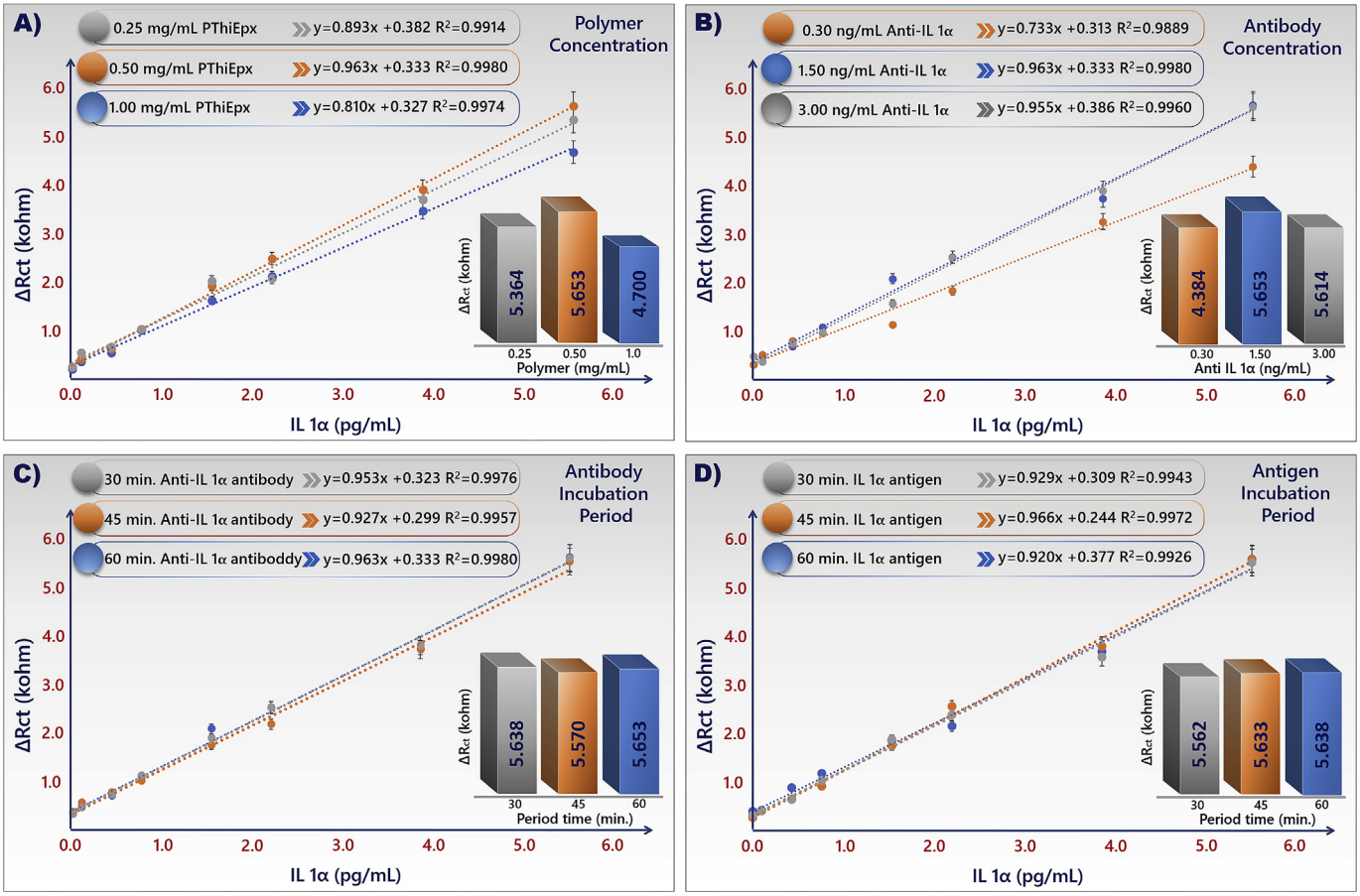

Fig. 3. Optimization of experiment results; polymer concentration (A), antibody concentration (B), antibody incubation period (C), antigen incubation period (D).

45 min, and 60 min incubation. As seen in Fig. 3C, the immunosensor signals were similar and 30-min incubation was enough to obtain good response. Also, longer incubation period did not increase the immunosensor response. Therefore, 30 min was employed for antibody incubation. Another important parameter that affect the immunosensor response was IL 1α antigen incubation period. The ITO/PThiEpx/anti-IL 1α/BSA bioelectrodes were separately immersed in PBS solution containing different concentrations of IL 1α antigen for three different amounts of time (30 min, 45 min, and 60 min). After 30-min incubation, the immunosensor signal was low. The maximum immunosensor response was attained after 45-min incubation. After 60-min incubation, there was no obvious variation on the signal, as shown in Fig. 3D. Hence, 45-min incubation was considered as the optimal IL 1α antigen incubation period.

3.5. Electrochemical responses of the developed immunosensor toward IL 1α antigens

Under optimal conditions, the proposed immunosensor was studied for quantification of IL 1α antigen by recording EIS spectra and CVs for different concentrations of IL 1α antigen. Fig. 4A and Fig. 4B show EIS spectra and CVs recorded for concentrations varying from 0.01 pg/mL to 5.5 pg/mL of IL 1α antigen, respectively. EIS analysis results indicated that R_{ct} values of the immunosensor increased with the increasing of IL 1α antigen level. In other words, with addition of IL 1α antigen, an insulator-like characteristic of biomolecule was formed, and this protein layer caused an increase in R_{ct} value. As the antigen concentration increased, the insulating characteristic increased and a result of this, charge transfer resistance increased further (Fig. 4A). However, peak currents decreased due to the same reason (Fig. 4B). As seen in Fig. 4C, the immunosensor displayed a wide linear detection range of 0.01 pg/mL-5.5 pg/mL with a low detection limit of 3.4 fg/mL (Signal/Noise: 3σ; σ is the standard deviation of the blank, n = 5) and a good sensitivity of 4.099 $pgmL^{-1}$ kohm cm^{-2}. This detection limit was more sensitive than ELISA. The linear regression equation of the proposed immunosensor was $\Delta R_{ct} = 0.959[IL\ 1\alpha] + 0.242$ ($R^2 = 0.9988$). For the analytical characterization of the biosensor, the bioelectrode measurements (n = 3) were performed with a single bioelectrode upon a single incubation with IL 1α antigen and the error bars were plotted considering standard deviation of the repeated R_{ct} measurements.

Apart from EIS and CV measurements, single frequency impedance measurement was performed to investigate the specific interaction between anti-IL 1α antibody and IL 1α antigen. This technique illustrates the time-dependent changes on the immunosensor surface at fixed frequency. The frequency value is defined from Bode Plot, because Nyquist plot does not include frequency. The Bode blot of this study is displayed in Fig. 4D. In order to perform SFI experiment, the potentiostat was set up at a fixed frequency of 12 Hz which was defined with the assistance of Bode plots. The SFI measurement was taken in PBS solution (50 mM, pH 7.4) containing IL 1α antigen. As seen in Fig. 4E, an increase was seen in impedance value. This increase verified that the specific interaction between anti-IL 1α antibody and IL 1α antigen.

3.6. Repeatability, reproducibility, selectivity, reusability and stability of the IL 1α immunosensor

Repeatability of the proposed immunosensor was examined by measuring EIS responses of 20 independent bioelectrodes after incubating them with 0.75 pg/mL of IL 1α antigen. The observed relative standard deviation (RSD%) of 4.37% indicated a good repeatability of the immunosensor. The reproducibility of the immunosensor was also

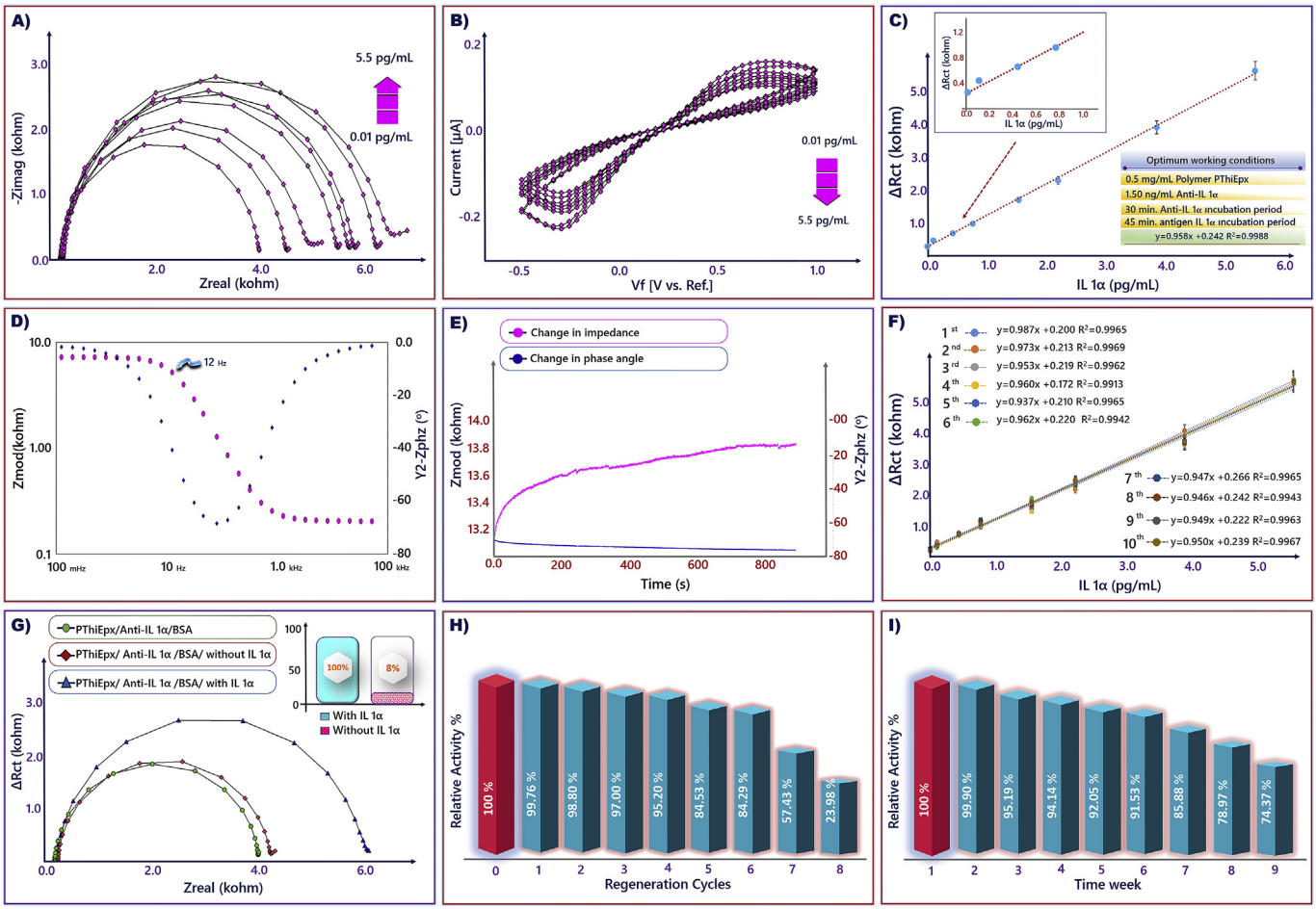

Fig. 4. EIS (A) and CVs (B) after incubating in IL 1α antigen solution with different concentrations ranging between 0.01 and 5.5 pg/mL, the calibration curve obtained by regressing R_{ct} values on IL 1α concentrations (C), Bode plot (D), single frequency impedance result (E), reproducibility of the immunosensor (F), selectivity of the immunosensor (G), regeneration experiment result (H), storage-stability of the immunosensor (I).

investigated. Under optimum conditions, the independent 10 immunosensors were prepared and the immunosensor signals were recorded. As seen in Fig. 4F, the RSD was only 1.53%. The results displayed that the immunosensor had an excellent reproducibility.

Selectivity is an important criterion in biosensing applications. The accurate detection of biomarkers in complex matrices such as serum, saliva and urine represents the success of the biosensor. To investigate the selectivity of the proposed biosensor, the proposed immunosensor tested with other cancer biomarkers such as neuron specific enolase, interleukin 1β, interleukin 8, and tumor necrosis factor α. In the first step of this experiment, the interference biomarkers (150 pg/mL) were mixed in PBS solution (50 mM pH 7.4). Then, ITO/PThiEpx/anti-IL 1α/BSA bioelectrode was immersed in this mixed solution (100 µL in microcentrifuge tube) and incubated there 45 min. After 45-min incubation period, impedimetric response of the bioelectrode was measured and a low response was measured (Fig. 4G, orange curve). This low response illustrated the negligible contribution of the nonspecific interactions. In the second step of this experiment, the interference biomarkers (150 pg/mL) and IL 1α antigen (1.5 pg/mL) were mixed in PBS solution (50 mM pH 7.4). Then, ITO/PThiEpx/anti-IL 1α/BSA bioelectrode was immersed in this mixed solution (100 µL in microcentrifuge tube) and incubated there 45 min. After 45-min incubation period, impedimetric response of the bioelectrode was measured and a high response was measured due to specific interaction between anti-IL 1α antibody and IL 1α antigen (Fig. 4G, blue curve). Consequently, this experiment confirmed the selectivity of the proposed immunosensor towards IL 1α antigen (Fig. 4G).

Regeneration of biosensor is an important advantage to reduce costs of biosensor and this feature accelerates the commercialization process. In general, the regeneration step is carried out under extreme conditions such as acidic and alkaline solution treatment. The reusability of the immunosensor was examined by immersion of ITO/PThiEpx/anti-IL 1α antibody/BSA/anti-IL 1α antigen electrode in 10 mM HCl solution for 5 min to eliminate IL 1α antigens from the immunosensor surface. After immersion in this regeneration solution, the immunosensor response was measured. Then, the immunosensor was dipped in IL 1α antigen solution, and specific interactions between anti-IL 1α antibody and IL 1α antigen were formed on the ITO substrate surface. After 7 cycles, the immunosensor had 54.73% of the initial impedance response (Fig. 4H). The signal decrease may result from unavoidable contamination and denaturation of anti-IL 1α antibodies. This result illustrated that the proposed biosensor was suitable for reusability. In addition, the storage stability of the immunosensor was also studied. After stored at 4 °C for 9 weeks, the immunosensor had 74.37% of the initial impedance response (Fig. 4I). Also, electrochemical immunosensor exhibited satisfactory stability.

3.7. Real sample analysis

The practical applicability of the proposed immunosensor was investigated by detection of IL 1α antigen in human serum. In the real sample application experiments, each sample measurement was repeated 2 times. Prior to analysis, the human serum samples were diluted with PBS buffer (20 fold; 50 µL human serum samples and 950 µL

Table 1
Human serum sample results.

Before antigen IL 1α (0.25 pg/mL) addition				After antigen IL 1α (0.25 pg/mL) addition				
Sample	Found by proposed immunosensor (pg/mL)	Standard Deviation	Coefficient Variation (%)	Total found by proposed immunosensor	Standard Deviation	Coefficient Variation (%)	Recovery (%)	Relative difference (%)
1	0.37	0.02	6.13	0.63	0.02	3.44	101.57	1.57
1	0.40			0.64			101.17	1.17
2	0.47	0.04	7.77	0.73	0.04	4.86	102.23	2.23
2	0.52			0.78			101.80	1.80
3	0.28	0.03	10.23	0.54	0.03	5.03	101.24	1.24
3	0.32			0.58			100.42	0.42
4	0.51	0.04	7.23	0.74	0.04	4.93	97.17	−2.83
4	0.46			0.69			96.98	−3.02
5	0.70	0.04	6.36	0.92	0.04	4.46	96.64	−3.36
5	0.64			0.86			96.88	−3.12

PBS buffer 50 mM pH 7.4). Then, ITO/PThiEpx/anti-IL 1α antibody/BSA bioelectrodes were immersed in these human serum samples (100 μL in microcentrifuge tube) and incubated there 45 min. After 45 min, the bioelectrodes were washed with ultrapure water and the EIS measurements were performed. In order to elucidate the analytical reliability of the suggested immunosensor, recovery experiments were performed. Firstly, known concentration of IL 1α antigen standards were spiked into human serum samples and ITO/PThiEpx/anti-IL 1α/BSA electrodes were incubated in these solutions under optimum conditions. After 45 min of incubation, the bioelectrodes were washed with ultrapure water and EIS was recorded in electrolyte solution. Recovery experiments illustrated that recovery yields of the EIS immunosensor from IL 1α antigen spiked human serum samples were ranging between 96.64% and 102.23% (Table 1). The successful results indicated that the proposed immunosensor could be applied to provide a possible application for IL 1α determination in human serum samples.

4. Conclusions

This study presented a label-free IL 1α immunosensor based on polymer PThiEpx modified disposable ITO electrode. The polymer PThiEpx could efficiently immobilize anti-IL 1α antibodies and act as an electrochemical biosensor interface. Use of the as-prepared polymer improved the electrochemical performance of the designed immunosensor. Our result suggests that this anti-IL 1α antibody functionalized immunosensor was simple, selective, and sensitive to the biorecognition of IL 1α antigens with a wide linear range (0.01 pg/mL-5.5 pg/mL) and low detection limit (3.4 fg/mL). Also, experimental results displayed that the designed immunosensor had high sensitivity, good repeatability, excellent stability, and acceptable reproducibility. Besides, the interference study proved that our immunosensor had high selectivity towards IL 1α antigen. In addition, the 'label-free' direct detection techniques had some advantages including ease of miniaturization and cost-effectiveness. Hence, the proposed immunosensor could be utilized as an optional technique for the determination of IL 1α antigen. Moreover, the practical applicability of the proposed immunosensor was tested in human serum and it had excellent recovery results. In conclusion, this immunosensor construction strategy provided a cost-effective and convenient operation and offered a great promise for the sensitive determination of cancer biomarkers.

CRediT authorship contribution statement

Muhammet Aydın: Investigation, Methodology, Software, Validation, Visualization, Writing - original draft, Writing - review & editing.

Declaration of competing interest

The authors declare that they have no known competing financial interests or personal relationships that could have appeared to influence the work reported in this paper.

Appendix A. Supplementary data

Supplementary data to this article can be found online at https://doi.org/10.1016/j.bios.2019.111675.

References

Austin, L.A., Osseiran, S., Evans, C.L., 2016. Analyst 141 (2), 476–503.
Aydın, E.B., Aydın, M., Sezgintürk, M.K., 2018a. Sens. Actuators, B 270, 18–27.
Aydın, E.B., Aydın, M., Sezgintürk, M.K., 2019a. Talanta 200, 387–397.
Aydın, E.B., Sezgintürk, M.K., 2019. Anal. Chim. Acta 1077, 129–139.
Aydın, M., Aydın, E.B., Sezgintürk, M.K., 2018b. Biosens. Bioelectron. 107, 1–9.
Aydın, M., Aydın, E.B., Sezgintürk, M.K., 2018c. Biosens. Bioelectron. 117, 720–728.
Aydın, M., Aydın, E.B., Sezgintürk, M.K., 2019b. Biosens. Bioelectron. 126, 230–239.
Aydın, M., Aydın, E.B., Sezgintürk, M.K., 2019c. Macromol. Biosci. 19, 1–12 1900109.
Bahadır, E.B., Sezgintürk, M.K., 2016. Analyst 141, 5618–5626.
Banas, A., Banas, K., Furgal-Borzych, A., Kwiatek, W., Pawlicki, B., Breese, M., 2015. Analyst 140 (7), 2156–2163.
Cervin Serrano, S., González Villareal, D., Aguilar-Medina, M., Romero-Navarro, J.G., Romero Quintana, J.G., Arámbula Meraz, E., Osuna Ramírez, I., Picos-Cárdenas, V., Granados, J., Estrada-García, I., 2014. Int. J. Genomics 2014.
Chen, Y., Yuan, P., Wang, A., Luo, X., Xue, Y., Zhang, L., Feng, J., 2019a. Biosens. Bioelectron. 126, 187–192.
Chen, Y., Wang, A., Yuan, P., Luo, X., Xue, Y., Feng, J., 2019b. Biosens. Bioelectron. 132, 294–301.
Clemens, G., Hands, J.R., Dorling, K.M., Baker, M.J., 2014. Analyst 139 (18), 4411–4444.
David, T., Dominic, J., Kumar, K.S., Vanaja, A., 2019. Polymer 175, 32–40.
de Mooij, C.E., Netea, M.G., van der Velden, W.J., Blijlevens, N.M., 2017. Blood 129 (24), 3155–3164.
Diaz, A., Rubinson, J., Mark, H., 1988. Electronic Applications. Springer, pp. 113–139.
Dinarello, C.A., Simon, A., Van Der Meer, J.W., 2012. Nat. Rev. Drug Discov. 11 (8), 633.
Feng, L., Zhu, C., Yuan, H., Liu, L., Lv, F., Wang, S., 2013. Chem. Soc. Rev. 42 (16), 6620–6633.
Festag, G., Steinbrück, A., Wolff, A., Csaki, A., Möller, R., Fritzsche, W., 2005. J. Fluoresc. 15 (2), 161–170.
Ghosh, A., Raha, S., Dey, S., Chatterjee, K., Chowdhury, A.R., Barui, A., 2019. Analyst 144 (4), 1309–1325.
Hamad, A.-W.R., Gaphor, S.M., Shawagfeh, M.T., Al-Talabani, N.G., 2011. Acad J Cancer 4 (2), 47–55.
Honore, P., Wade, C.L., Zhong, C., Harris, R.R., Wu, C., Ghayur, T., Iwakura, Y., Decker, M.W., Faltynek, C., Sullivan, J., 2006. Behav. Brain Res. 167 (2), 355–364.
Janmanee, R., Chuekachang, S., Sriwichai, S., Baba, A., Phanichphant, S., 2012. J. Nanotechnol. 2012.
Katz, E., Willner, I., 2004. Angew. Chem. Int. Ed. 43 (45), 6042–6108.
Kitagawa, T., Hirota, S., 2006. Handbook of Vibrational Spectroscopy. Wiley, New York.
Korostoff, A., Reder, L., Masood, R., Sinha, U.K., 2011. Oral Oncol. 47 (4), 282–287.
Kuhar, N., Sil, S., Verma, T., Umapathy, S., 2018. RSC Adv. 8 (46), 25888–25908.
Li, J., Gao, H., Chen, Z., Wei, X., Yang, C.F., 2010. Anal. Chim. Acta 665 (1), 98–104.
Lisdat, F., Schäfer, D., 2008. Anal. Bioanal. Chem. 391 (5), 1555.
Malinauskas, A., Malinauskiene, J., Ramanavičius, A., 2005. Nanotechnology 16 (10), R51.
Mishra, R., 2012. Oral Oncol. 48 (7), 578–584.
Moon, J.-M., Thapliyal, N., Hussain, K.K., Goyal, R.N., Shim, Y.-B., 2018. Biosens. Bioelectron. 102, 540–552.

Neises, B., Steglich, W., 1978. Angew. Chem., Int. Ed. Engl. 17 (7), 522–524.
Oh, J., Lee, J.-H., Koo, J.C., Choi, H.R., Lee, Y., Kim, T., Luong, N.D., Nam, J.-D., 2010. J. Mater. Chem. 20 (41), 9200–9204.
Palecek, E., Bartosik, M., 2012. Chem. Rev. 112 (6), 3427–3481.
Panikkanvalappil, S., Garlapati, C., Hooshmand, N., Aneja, R., El-Sayed, M.A., 2019. Chem. Sci. 10, 4876–4882.
Pänke, O., Balkenhohl, T., Kafka, J., Schäfer, D., Lisdat, F., 2007. Biosensing for the 21st Century. Springer, pp. 195–237.
Park, J.E., Barbul, A., 2004. Am. J. Surg. 187 (5), S11–S16.
Pilo, M., Farre, R., Lachowicz, J.I., Masolo, E., Panzanelli, A., Sanna, G., Senes, N., Sobral, A., Spano, N., 2018. J. Anal. Methods Chem. 2018.
Plante, M.-P., Bérubé, E.v., Bissonnette, L., Bergeron, M.G., Leclerc, M., 2013. ACS Appl. Mater. Interfaces 5 (11), 4544–4548.
Polanska, H., Raudenska, M., Gumulec, J., Sztalmachova, M., Adam, V., Kizek, R., Masarik, M., 2014. Oral Oncol. 50 (3), 168–177.
Rahman, M., Kumar, P., Park, D.-S., Shim, Y.-B., 2008. Sensors 8 (1), 118–141.
Ramanavičius, A., Ramanavičienė, A., Malinauskas, A., 2006. Electrochim. Acta 51 (27), 6025–6037.
Russo, N., Bellile, E., Murdoch-Kinch, C.A., Liu, M., Eisbruch, A., Wolf, G.T., D'silva, N.J., 2016. Oral surgery, oral medicine. oral pathology and oral radiology 122 (4), 483–490 e481.
Shi, Y., Wang, A., Yuan, P., Zhang, L., Luo, X., Feng, J., 2018. Biosens. Bioelectron. 111, 47–51.
Tang, J., Tang, D., Niessner, R., Chen, G., Knopp, D., 2011. Anal. Chem. 83 (13), 5407–5414.
Tao, Z., Tehan, E.C., Bukowski, R.M., Tang, Y., Shughart, E.L., Holthoff, W.G., Cartwright, A.N., Titus, A.H., Bright, F.V., 2006. Anal. Chim. Acta 564 (1), 59–65.
Vashist, S.K., Luong, J.H., 2018. Handbook of Immunoassay Technologies: Approaches, Performances, and Applications. Academic Press.
Védrine, C., Fabiano, S., Tran-Minh, C., 2003. Talanta 59 (3), 535–544.
Wang, R., Liu, W., Wang, A., Xue, Y., Wu, L., Feng, J., 2018. Biosens. Bioelectron. 99, 458–463.
Wang, Y., Hasebe, Y., 2009. Talanta 79 (4), 1135–1141.
Wu, B.-y., Wang, Y.-y., Li, J., Song, Z., Huang, J.-d., Wang, X.-s., Chen, Q., 2006. Talanta 70 (3), 485–488.
Wu, H., Liu, G., Wang, J., Lin, Y., 2007. Electrochem. Commun. 9 (7), 1573–1577.
Xu, Y., Long, G., Huang, L., Huang, Y., Wan, X., Ma, Y., Chen, Y., 2010. Carbon 48 (11), 3308–3311.
Zhang, B., Tang, D., Liu, B., Cui, Y., Chen, H., Chen, G., 2012. Anal. Chim. Acta 711, 17–23.
Zhang, S., Zhang, L., Zhang, X., Yang, P., Cai, J., 2014. Analyst 139 (14), 3629–3635.
Zhang, Y., Ren, W., 2013. Anal. Methods 5 (13), 3379–3385.